

## **Inhibitive effect of 6-dibutylamino-1,3,5-triazine-2,4-dithiolmonosodium as a corrosion inhibitor for SUS304 stainless steel in hydrochloric acid solution**

*Qian Zhao*

Shaanxi Key Laboratory of Disaster Monitoring and Mechanism Simulation, Baoji University of Arts and Sciences, Baoji, Shaanxi 721013, P.R. China

E-mail: [qianzhao@bjwlxy.cn](mailto:qianzhao@bjwlxy.cn)

*Received:* 19 October 2018 / *Accepted:* 5 December 2018 / *Published:* 5 January 2019

---

Stainless steels have been used extensively in various fields while corrosion can brought serious problems to their functionality. The inhibition effect of 6-dibutylamino-1,3,5-triazine-2,4-dithiolmonosodium (DBN) on SUS304 stainless steel corrosion in 1.0 M HCl was studied by means of electrochemical impedance spectroscopy (EIS), potentiodynamic polarization, cyclic voltammeter (CV) and scanning electron microscopy (SEM) techniques. Results from electrochemical measurements showed that the corrosion inhibition performance of DBN was effective, and the protection efficiency was up to 99.82%. Adsorption of DBN inhibitors on stainless steel surface followed Langmuir's adsorption isotherm at 30 °C. Further, morphology observation suggested that the stainless steel was well protected by DBN inhibitor.

---

**Keywords:** Stainless steel, Triazinedithiols, Corrosion inhibitor, Polarization

### **1. INTRODUCTION**

Stainless steels are widely applied in various fields, however, corrosion can brought severe problems to their functionality. The research of corrosion inhibition of stainless steel employing effective inhibitors in acidic media, containing HCl or H<sub>2</sub>SO<sub>4</sub> in particular, is one of the challenging topic of present research in various industries including acid oil-well acidizing, chemical cleaning, descaling and pickling [1-3]. Stainless steel corrosion is induced by the chemical or electrochemical reactions between its surface and corrosive environments. The extensive localized corrosion on stainless steel materials can result in serious damage of functionality [4, 5]. For instance, corrosion damage can lead to leakage of fluids or gases, so special attention should be paid to protect pipelines and tanks. More dangerously, corrosion and subsequent failure would induce a loss of strength of the structure [6]. Thus, efforts have been made to hinder the corrosion of stainless steel [7-9] and the employment of organic inhibitors has

been regarded as the most common approach to protect the integrity of stainless steel surface [10-12]. The organic molecules can absorb on the surface of stainless steel and block the active corrosion spots, in this way, the corrosion rate is reduced [13]. However, research on the cost-effective, low-toxicity and environmentally friendly corrosion inhibitors with high corrosion inhibition efficiency for stainless steel is urgently needed.

Triazinedithiol and its monosodium salt, with high reactivity, low cost, high solubility and without unfavorable mercaptan smell and toxicity, have been used in many fields acted as environmentally friendly compounds [14-16]. It was reported earlier that the special tautomer of thiol–thione with highly electronegative atoms like S and O, and the N-containing heterocyclic conjugate system, favor the adsorption of triazinedithiol molecules on metallic surface [17]. Whereas the study on triazinedithiol inhibitor for stainless steel is seldom reported.

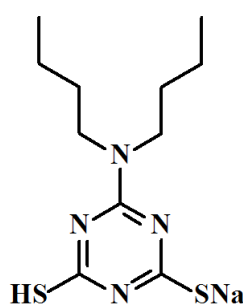


**Figure 1.** Molecule structures of 6-dibutylamino-1,3,5-triazine-2,4-dithiolmonosodium (DBN)

In present study, 6-dibutylamino-1,3,5-triazine-2,4-dithiolmonosodium (DBN, Figure 1) was synthesized and acted as corrosion inhibitor for SUS304 stainless steel, and the potentiodynamic polarization and electrochemical impedance spectroscopy (EIS) are employed to evaluate the inhibition efficiency and mechanism of DBN monolayers on the SUS304 stainless steel surface in 1.0 M HCl solution. The protective performance was further investigated by electrochemical measurement and SEM technique. Besides, the absorption behavior of DBN on stainless steel surface was also fitted by Langmuir adsorption isotherm.

## 2. EXPERIMENTAL

### 2.1. Materials and sample preparation

The elemental composition (wt.%) of SUS304 stainless steel employed in present study is shown below: 18.18% Cr, 8.48% Ni, 2% Mn, 0.75% Si, 0.03% C, 0.12% N, 0.03% S, 0.045% P and the remainder is Fe. Prior to each measurement, the specimen was polished with abrasive papers (80-2000 grit size). Then the polished samples were rinsed with distilled water, dried in air, and degreased with acetone in turn. After that, the margin part of each sample was covered with epoxy resin, forming a 1×1 cm<sup>2</sup> area in the middle of the stainless steel surface. The aggressive solution of 1 M HCl was prepared by dilution of analytical grade HCl with double distilled water. The inhibitor concentrations varied from

0.01 to 0.5 mM. DBN was synthesized through the chemical reaction between NaSH and 6-N,N-dibutylamino-1,3,5-triazine-2,4-dichloride [15].

## 2.2 Electrochemical measurements

All the electrochemical measurements are performed using the Electrochemical Workstation (Model: Chenhua Instruments Co., Ltd., Shanghai). The platinum electrode is used as auxiliary electrode, and saturated calomel electrode (SCE) is reference electrodes. The stainless steel specimens with 1 cm<sup>2</sup> area exposed constitute the working electrodes.

Prior to each measurement, OCP (all the electrodes were immersed in solution for 60 min to obtain a constant potential) was established first, then the polarization measurements were performed at a scan rate of 0.5 mV/s. The polarization curves for SUS304 stainless steel samples in the test solution with and without various concentrations of inhibitors were recorded from -250 to +250 mV versus OCP. Electrochemical impedance spectroscopy (EIS) measurement was carried out at steady state open circuit potential disturbed with amplitude of 10mV ac sine wave in the frequency range 100 kHz to 10 mHz. Cyclic voltammetry (CV) was carried out between the potential region from -0.65 V to +1.5 V at a 20 mV/s in 0.1 M HCl solution. In order to demonstrate reasonable reproducibility, all tests were repeated at least three times under the same conditions.

## 2.3 Scanning Electron Microscopy (SEM)

SEM (JSM-6360LV, JEOL, Tokyo, Japan) technique was carried out to further study the corrosion resistance performance of DBN. Surfaces morphologies of SUS304 stainless steel after immersing in 1 M HCl for 12 h in absence and presence of DBN inhibitor were observed and recorded. The accelerating voltage was 20 kV.

# 3. RESULTS AND DISCUSSION

## 3.1. The curves of open circuit potential (OCP) versus time for different concentration of DBN.

The open circuit potentials ( $E_{oc}$ ) of stainless steel in 1 M HCl solution in the absence and presence of different concentrations of DBN was monitored for 60 min to achieve the free corrosion potential or the quasi-stationary  $E_{oc}$  value. The OCP transients obtained for DBN are shown in Fig. 2. Except for two cases (stainless steel without inhibitor and with a 0.1 mM DBN added), stainless steel potential drifts with time in the negative direction until it tends to stabilize. The positive shift of potentials is related to continuous dissolution of stainless steel sample in hydrogen chloride solution due to the non-protective nature of its native surface film [18]. Compared with the Blank group, the stabilized  $E_{oc}$  becomes significantly more negative with the presence of DBN inhibitor. These results may be interpreted on the basis of forming protective layer from the adsorbed DBN molecules on the active cathodic sites of the stainless steel surface, which inhibit the corrosion process of stainless steel. Similar OCP results were observed by Heakal, in which an adhere layer of thiadiazole derivatives inhibitor molecules on the surface of steel is proposed to account for their inhibitive action [19]. The presence of 0.25 mM DBN

makes its surface potential more negative than others. Therefore, the lower OCP could be associated to the higher amount of DBN molecules absorbed on metal surface.

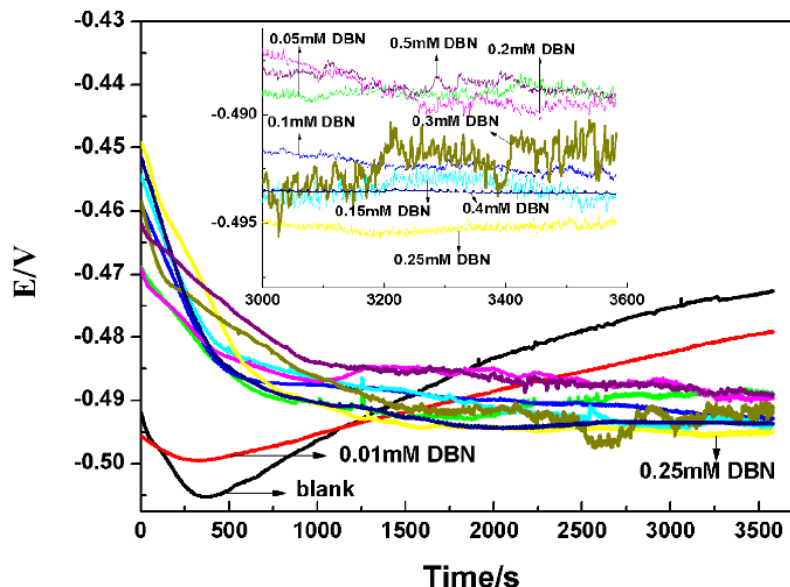


**Figure 2.** Open circuit potential curves of SUS304 stainless steel in 1 M HCl in absence and presence of different concentrations of DBN added, respectively.

### 3.2. Potentiodynamic Polarization Measurements.

Potentiodynamic polarization profiles for stainless steel in 1 M HCl solution in the absence and presence of different concentrations of DBN are presented in Figure 3. The concentrations used were ranged from 0.01 mM to 0.5 mM. Table 1 exhibited the corrosion kinetics parameters including corrosion potential ( $E_{corr}$ ), corrosion current density ( $I_{corr}$ ) and cathodic and anodic Tafel slopes ( $\beta_a, \beta_c$ ), where the inhibition efficiency  $\eta_p(\%)$  was calculated by:

$$\eta_p(\%) = \frac{I_{corr}^0 - I_{corr}^i}{I_{corr}^0} \times 100 \tag{1}$$

Where  $I_{corr}^0$  and  $I_{corr}^i$  are the corrosion current densities of stainless steel in the absence and the presence of inhibitor.

From Figure 3, it is clearly observed that the cathodic currents were significantly decreased with the presence of DBN inhibitor and  $E_{corr}$  shifted to the negative potentials after the addition of DBN compounds, which indicated that the adsorption of DBN molecules on the active sites lead to a great reduction of the hydrogen evolution reaction, while its inhibition effect on the anodic dissolution was relatively unobvious. In general, both the cathodic and anodic curves were shifted towards lower values with the concentration of DBN increased. From Table 1, it is obviously seen that when more DBN inhibitor was added in to the corrosive solution, the corrosion current density decreased and the inhibition efficiency increased. When the adding amount of DBN reached 0.25 mM, the lowest  $I_{corr}$  values of  $10.66 \mu A \cdot cm^{-2}$  was obtained and the inhibition efficiency attained 99.82% (Table 1). This indicates that when the concentration of DBN is around 0.25 mM, the adsorption of the inhibitor

molecules on the SUS304 stainless steel surface reaches an equilibrium state of saturation. If the concentration of the inhibitor continues to increase, the saturated adsorption film will be influenced by the molecular interaction. As a result, the adsorption capacity and stability of the inhibitor molecules would be reduced, and the corrosion inhibition efficiency shows a downward trend. In general, a compound is regarded as a anodic or cathodic type when the displacement in  $E_{\text{corr}}$  is greater than 85 mV, or else inhibitor is considered as a mixed type [20]. For DBN, the maximum displacement of  $E_{\text{corr}}$  values is 41.63 mV, which suggested that DBN belonged to mixed-type inhibitors, mainly inhibiting the cathodic processes (Table 1).

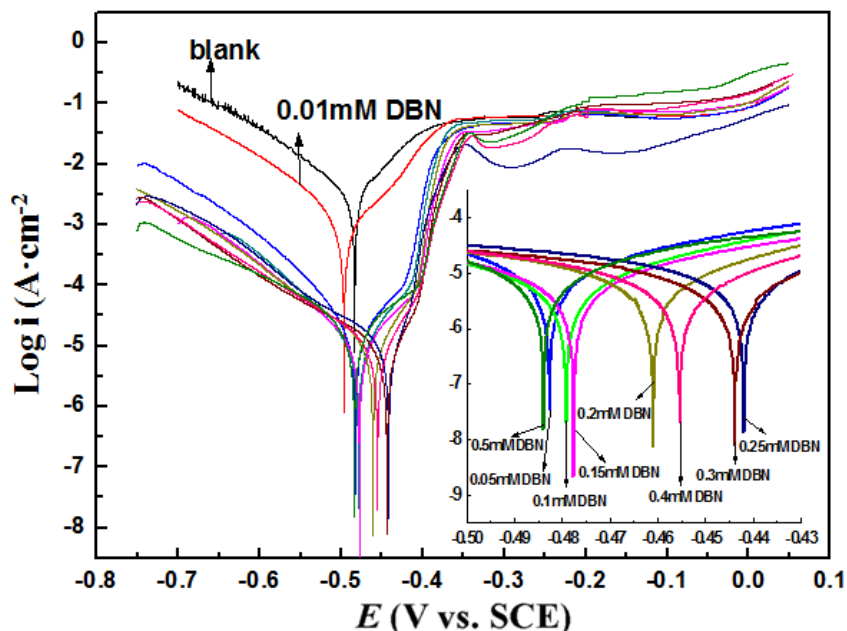


**Figure 3.** Tafel plots for SUS304 stainless steel in 1 M HCl in absence and presence of different concentrations of DBN.

**Table 1.** Tafel polarization parameters of the corrosion for SUS304 stainless steel in 1M HCl in absence and presence of different concentrations of DBN.

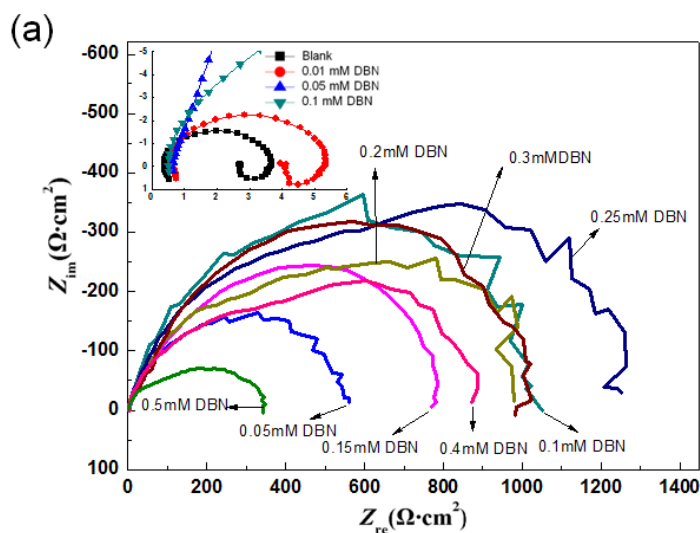
$C_{\text{inhibitor}}$ (mM)	$\beta_a$ (mV dec <sup>-1</sup> )	$\beta_c$ (mV dec <sup>-1</sup> )	$I_{\text{corr}}$ (A cm <sup>-2</sup> )	$-E_{\text{corr}}$ (mV/SCE)	$\eta_p$ (%)
Blank	67.7	257	$5.97 \times 10^{-3}$	484	—
0.01	169	123	$2.03 \times 10^{-3}$	497	65.96
0.05	88.2	72.8	$2.06 \times 10^{-5}$	483	99.66
0.10	82.4	113	$1.65 \times 10^{-5}$	479	99.72
0.15	90.9	104	$1.42 \times 10^{-5}$	478	99.76
0.20	68.0	133	$1.42 \times 10^{-5}$	461	99.76
0.25	40.1	120	$1.07 \times 10^{-5}$	442	99.82
0.30	59.2	153	$1.13 \times 10^{-5}$	444	99.81
0.40	66.4	125	$1.17 \times 10^{-5}$	455	99.80
0.50	180	191	$3.96 \times 10^{-5}$	484	99.34

### 3.3 Electrochemical Impedance Spectroscopy (EIS) Measurements

The Nyquist representations of impedance behavior of stainless steel in 1 M HCl with and without addition of various concentrations of DBN are given in Figure 4. Obviously, all impedance spectra present a single slightly depressed semi-circle, suggesting a non-ideal capacitive behavior of the electrochemical solid/liquid interface. The deviation from pure semi-circle behavior (frequency depression) is caused by roughness and inhomogeneity of the surface during corrosion [21].

It can be observed that the diameter of capacitive loop is enlarging gradually with adding different concentrations of DBN, which indicates that the inhibitor increases the resistance to charge transfer. This infers DBN acts via adsorption the organic constituents at the metal-solution interface. The adsorption of the constituents on the electrode surface decreases its electrical capacity by displacing the water molecules and other ions originally adsorbed on the surface [22]. The adsorbed DBN molecule forms a protective film on the electrode surface and consequently become a barrier to hinder the mass and charge transfer, resulting in an increase in the inhibition efficiency. The adsorbed layer may produced by the interaction between either the lone pairs of electrons on sulphur atoms or conjugated double bond or both present in DBN and the vacant d-orbital of iron in stainless steel. Moreover the obtained impedance spectra consist of one capacitive loop, which indicates that adsorption occurs by simple surface coverage and DBN as a primary interface inhibitor.

From figure 4, it can be observed that the semicircle diameter becomes largest when the DBN concentration at 0.25 mM, indicating that adsorption of inhibitors reach the maximum capacity and form a most compact and stable monolayer on metal surface. The corresponding Bode and phase angle plots are illustrated in Figure 4b and 4c. The Bode plots show that the impedace value over the whole frequency range increases greatly with increasing the DBN concentration. Besides, a larger  $|Z|$  value demonstrates a better protection performance (Figure 4b). The single narrow peaks in the phase-angle plots indicate a single time constant for the corrosion process at the metal-solution interface. The increase in the peak heights indicates a more capacitive response of the interface due to the presence of inhibitor molecules at the interface [23].



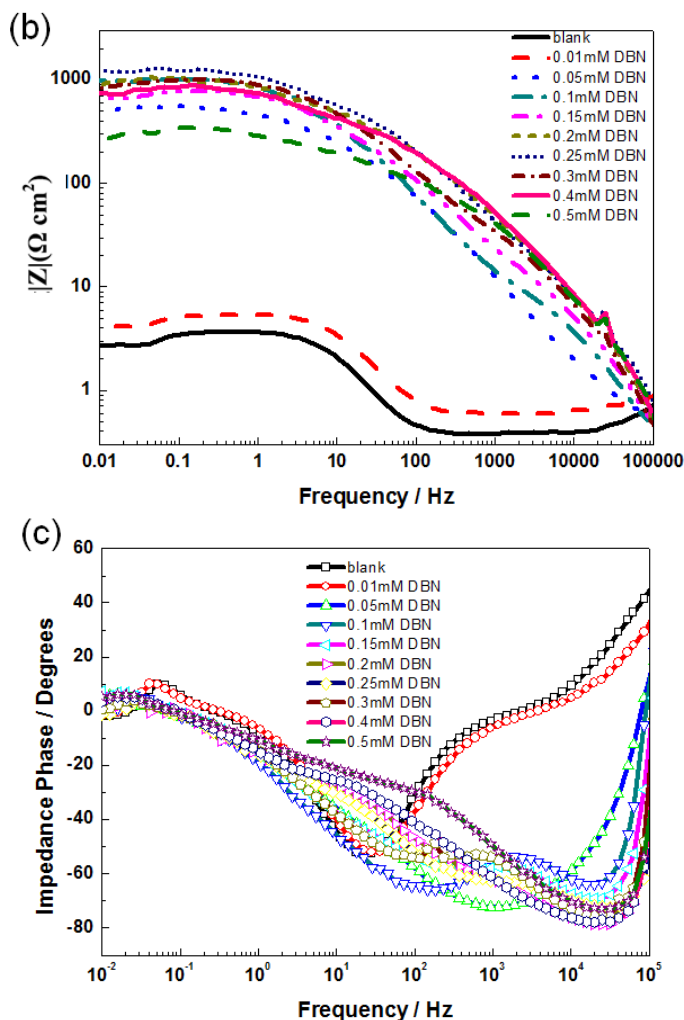


**Figure 4.** Nyquist diagrams (a), bode plots (b) and phase angleplots (c) for SUS304 stainless steel in 1 M HCl in absence and presence of different concentrations of DBN.

According to the appearance of phase angle plots (Figure 4c), more larger value of the phase angle was observed with the increasing concentration of DBN. In other words, a increase adsorption amount of DBN molecules at the SUS304 stainless steel surface results superior inhibition behavior.

### 3.4. Cyclic voltammogram

Cyclic voltammetry (CV) was applied to study the compactness of DBN modified stainless steel surface. To establish the optimum inhibitor concentration in the formation of absorbed film, different range of 0~0.5 mM DBN was used in the CV test. It can be seen that one obvious oxidation peaks at 0.99V in the positive scan and a reduction peak occur at -0.49V in the reverse sweep for bare stainless steel. The oxidation peak may related to the formation of  $\text{FeCl}_2$  ad-layer and the reduction peak is concerned with the reduction of the  $\text{FeCl}_2$  layer and soluble iron complex [24]. The size of the peak current can reflects the quantity of transferred electron during electrochemical reactions. When DBN inhibitor was presented, all anodic oxidation peaks were decreased obviously. Anodic oxidation peak

occurred at 0.97V was minimized when DBN was at a 0.25 mM concentration. This might be attributed to the adsorption of DBN molecules on copper surface to form the compact protective layer which make a better barrier to block charge or reactant ion transmission. Furthermore, the peak potentials shift in both directions. These observations suggest that DBN absorbed layer on stainless steel surface can strongly inhibits the oxidation processes of stainless steel and 0.25 mM was the optimum inhibitor concentration.

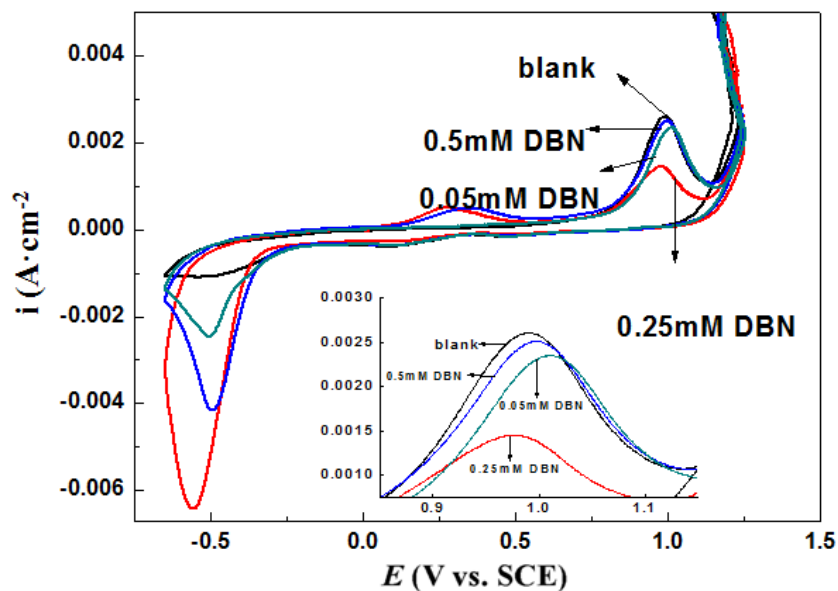


**Figure 5.** Cyclic voltammogram of SUS304 stainless steel in 1 M HCl in absence and presence of different concentrations of DBN.

### 3.5. Adsorption isotherm

Fundamental information on the adsorption of inhibitor on metal surface can be provided by adsorption isotherm. To determine the adsorption mode, various isotherms (Frumkin, Langmuir, Temkin, Freundlich, Frumkin and Flory-Huggins) were tested and the Langmuir mode should be the best (Figure 6). The characteristic of Langmuir adsorption isotherm is given by following equation[25] :

$$\frac{c}{\theta} = \frac{1}{K_{ads}} + c \tag{2}$$

where c is the concentration of inhibitor,  $K_{ads}$  is the adsorptive equilibrium constant and  $\theta$  is the surface coverage equal to inhibition efficiency  $\eta_w/100$ . Plots of  $C/\theta$  against C yield straight line as shown in Figure 6. Both linear regression coefficients ( $R^2$ ) and slope are quite equal to 1, indicating that DBN molecules formed a single molecule adsorbed layer on the stainless steel surface, and there was no interaction between absorbed molecules. Gibbs free energy ( $\Delta G_{ads}$ ) could be calculated with the following equation [26]:

$$\Delta G_{ads} = -RT \ln(55.5K_{ads}) \tag{3}$$

where R is the gas equilibrium constant, T is the temperature, the value 55.5 is the molecular concentration of water in solution.



In Figure 6, the intercept on the vertical axis is the value of  $1/K_{ads}$ , which is  $1.31 \times 10^{-3}$ . Then according to Eq. (3), we calculated the  $\Delta G_{ads} = -22.4$  kJ/mol at 303K. The negative values of  $\Delta G_{ads}$  suggested that the adsorption of DBN molecule was a spontaneous process. Generally, values of  $\Delta G_{ads}$  up to -20 kJ/mol, the types of adsorption were regarded as physisorption, the inhibition acts due to the electrostatic interactions between the charged molecules and the charged metal, while values around -40 kJ/mol or smaller are associated with chemisorption as a result of sharing or transfer of electrons from organic molecules to the metal surface to form a coordinate type of bond (chemisorption) [27]. Therefore, the process of DBN molecules adsorbed on the surface of stainless steel was not a single physical adsorption or chemisorption, but the result of the combined action of this two kinds of adsorption.

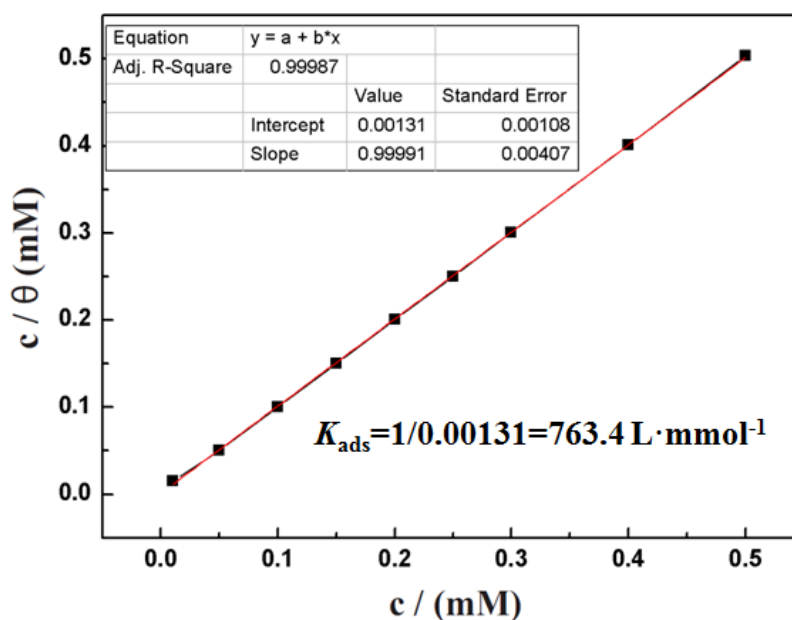
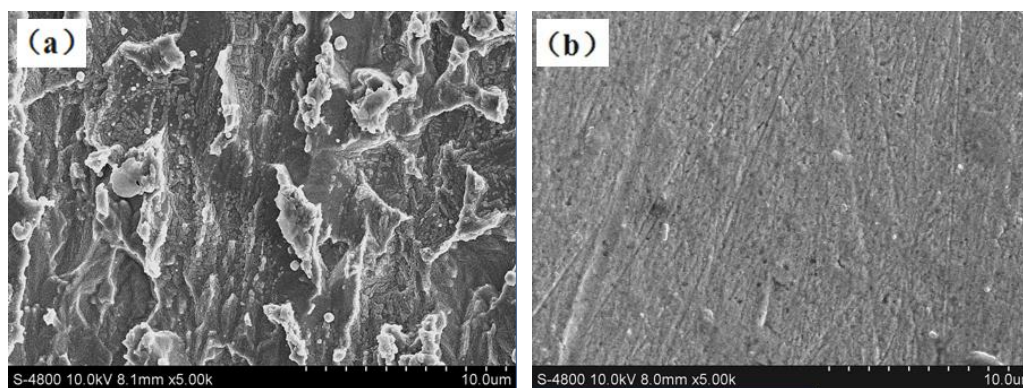


Figure 6. Langmuir isotherm adsorption isotherm of DBN in 1 M HCl solution.

### 3.6 Surface Morphology

SEM technique was carried out to further study the corrosion resistance performance of DBN, and the observation images of SUS304 stainless steel surface after immersing in 1 M HCl for 12 h in absence and presence of 0.25 mM DBN are given in Figure 6. In the absence of DBN, the metal plate presented a very rough surface with deep cracks (Figure 7a), which indicates a severe dissolution and strong damage of stainless steel in contact with aggressive solution. In contrast, a relative smooth surface with a few small holes is exhibited in Figure 7b, which revealed that the dissolution rate of stainless steel was effectively inhibited by DBN. It can be inferred that the regular distribution of DBN molecules absorbed on the surface of stainless steel forms a relatively compact protective layer, resulting in a decrease in the contact between HCl molecules and SUS304 stainless surface.



**Figure 7.** SEM images of SUS304 stainless steel after 12 h of immersion in 1 M HCl (a) without and (b) with 0.25 M DBN.

#### 4. CONCLUSIONS

DBN acts as a good inhibitor for corrosion of stainless steel in 1.0 M HCl solution. Results from potentiodynamic polarization, EIS and CV test all showed that 0.25 mM is the optimal concentration of DBN with corrosion inhibition efficiency reached 99.82%. Adsorption of DBN on stainless steel surface obeys the Langmuir isotherm at 30°C, and the process of DBN molecules adsorbed on the surface of stainless steel was the result of the combined action of the chemical and physical adsorption.

#### ACKNOWLEDGEMENTS

This research was supported by the Natural Science Basic Research Plan in Shaanxi Province of China (No. 2018JQ5191), the Young Talent fund of University Association for Science and Technology in Shaanxi, China (No. 20180419) and the Doctoral Scientific Research Foundation of Baoji University of Arts and Sciences (No. ZK2018044).

#### References

1. M. Mehdipour, B. Ramezanzadeh and S.Y. Arman, *J. Ind. Eng. Chem.*, 21 (2015) 318.
2. C. Cardona, A.A. Torres, J.M. Miranda-Vidales, J.T. Perez, M.M. Gonzalez-Chavez, H. Herrera-Hernandez and L. Narvaez, *Int. J. Electrochem. Sci.*, 10 (2015) 1966.
3. R.Y. Khaled and A.M. Abdel-Gaber, *Prot. Met. Phys. Chem.*, 53 (2017) 956.
4. A. Bautista, S.M. Alvarez and F. Velasco, *Mater. Corros.*, 66 (2015) 347.
5. N. Soltani, N. Tavakkoli, M.K. Kashani, A. Mosavizadeh, E.E. Oguzie and M.R. Jalali, *J. Ind. Eng. Chem.*, 20 (2014) 3217.
6. N. Goudarzi and H. Farahani, Investigation on 2-mercaptobenzothiazole behavior as corrosion inhibitor for 316-stainless steel in acidic media, *Anti-Corros. Method M.*, 61 (2014) 20.
7. A.S. Fouda, S.M. Rashwan and H.A. Abo-Mosallam, *Desalin. Water Treat.*, 52 (2014) 5175.
8. Y. Huang, D.K. Sarkar, D. Gallant and X.G. Chen, *Appl. Surf. Sci.*, 282 (2013) 689.
9. M.N. El-Haddad and K.M. Elattar, *Res. Chem. Intermed.*, 39 (2013) 3135.
10. S.M.A. Hosseini, M. Salari and M. Ghasemi, *Mater. Corros.*, 60 (2009) 963.
11. P. Henry, J. Takadoum and P. Berçot, *Corros. Sci.*, 51 (2009) 1308.
12. X.X. Sheng, Y.P. Ting and S.O. Pehkonen, *Adv. Mat. Res.*, 20-21 (2007) 379.
13. L. Narvaez, E. Cano and D.M. Bastidas, *J. Appl. Electrochem.*, 35 (2005) 499.

14. Q. Zhao, T.T. Tang, P.L. Dang and F. Wang, *Metals*, 7 (2017) 44.
15. F.Wang, J. Liu, Y. Li and R. Fan, *Int. J. Electrochem. Sci.*, 7 (2012) 3672.
16. J.A. Pinson, Z. Zheng Z and M.S. Miller MS., *Acs Med. Chem. Lett.*, 4 (2013) 206.
17. Z.X. Kang, K. Mori, and Y. Oishi, *Surf. & Coat. Tech.*, 195(2005)162.
18. B. Jegdić, D.M. Dražić and J.P. Popić, *Corros. Sci.*, 50 (2008) 1235.
19. E.T. Heakal, A.S. Fouda and M.S. Radwan, *Mater. Chem. Phy.*, 125 (2011) 26.
20. J.A. Pinson, Z. Zheng Z and M.S. Miller MS., *Acs Med. Chem. Lett.*, 4 (2013) 206.
21. L. Guo, S. Zhu and S. Zhang, *Ind.Engi.Chem.*, 24 (2015) 174.
22. Z.X. Kang, K. Mori, and Y. Oishi, *Surf. & Coat. Tech.*, 195 (2005) 162.
23. P. Mourya, S. Banerjee and M.M. Singh, *Corros. Sci.*, 85 (2014) 352.
24. S. Shahabi, P. Norouzi and M.R. Ganjali, *Russ. J. Electrochem.*, 51 (2015) 833.
25. D. Jones and E. Birks, *J. Chem. Soc.*, 145-147 (1951) 1127.
26. A. Dąbrowski, *Adv. Colloid Interface Sci.*, 93 (2001) 135.
27. Z. Szklarska-Smialowska and J. Mankowski, *Corros. Sci.*, 18 (1978) 953.

© 2019 The Authors. Published by ESG ([www.electrochemsci.org](http://www.electrochemsci.org)). This article is an open access article distributed under the terms and conditions of the Creative Commons Attribution license (<http://creativecommons.org/licenses/by/4.0/>).